

# Decelerating Effect of Alkynes in the Oxidative Addition of Phenyl Iodide to Palladium(0) Complexes in Palladium-Catalyzed Multicomponent Reactions and Sonogashira Reactions

Christian Amatore,<sup>\*,[a]</sup> Samia Bensalem,<sup>[a]</sup> Said Ghalem,<sup>[b]</sup> Anny Jutand,<sup>\*,[a]</sup> and Youcef Medjour<sup>[a]</sup>

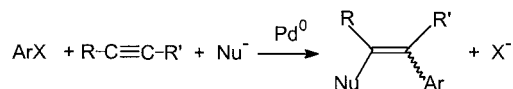
**Keywords:** Alkynes / Kinetics / Mechanism / Oxidative addition / Palladium

The oxidative addition of PhI to  $[\text{Pd}^0(\text{PPh}_3)_4]$  in DMF is slower when performed in the presence of the terminal alkynes ( $\text{PhC}\equiv\text{CH}$ ,  $\text{EtO}_2\text{C}-\text{C}\equiv\text{CH}$ ) that are reagents in palladium-catalyzed Sonogashira or multicomponent reactions. The concentration of the reactive  $[\text{Pd}^0(\text{PPh}_3)_2]$  complex decreases because of its partial coordination to the alkyne to form  $[(\eta^2-\text{RC}\equiv\text{CH})\text{Pd}^0(\text{PPh}_3)_2]$  ( $\text{R} = \text{Ph}$ ,  $\text{EtCO}_2$ ), which is in equilibrium with  $[\text{Pd}^0(\text{PPh}_3)_2]$ . The complex  $[(\eta^2-\text{PhC}\equiv\text{CH})\text{Pd}^0(\text{PPh}_3)_2]$  was found to be unreactive whereas  $[(\eta^2-\text{EtO}_2\text{C}-\text{C}\equiv\text{CH})\text{Pd}^0(\text{PPh}_3)_2]$  was found to be the unique reactive com-

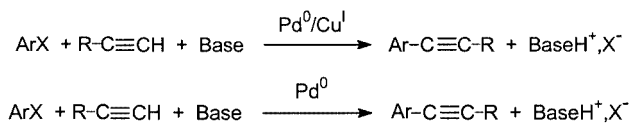
plex at high concentrations of  $\text{EtO}_2\text{C}-\text{C}\equiv\text{CH}$ . As has been reported for alkenes, terminal alkynes play an unexpected role because they interfere in the oxidative addition before their usual reactions in the carbopalladation and transmetalation steps that follow it. Decreasing the rate of the fast oxidative addition with PhI may promote the efficiency of the catalytic cycle by bringing its rate closer to that of the slower carbopalladation or transmetalation steps.  
(© Wiley-VCH Verlag GmbH & Co. KGaA, 69451 Weinheim, Germany, 2004)

## Introduction

Alkynes may be activated through palladium-catalyzed reactions such as three-component reactions (Scheme 1)<sup>[1–3]</sup> or Sonogashira reactions (terminal alkynes; Scheme 2).<sup>[4,5]</sup>



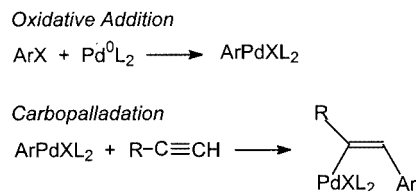
Scheme 1



Scheme 2

In multicomponent reactions (Scheme 1),<sup>[1–3]</sup> the alkynes react in the second step of the catalytic cycle (*carbopalladation* step), i.e., with the arylpalladium(II) complex that was

generated in the *oxidative addition* of the aryl halide to a palladium(0) complex (Scheme 3).



Scheme 3

The mechanism of the Sonogashira reactions has not yet been established clearly. In the process using a copper co-catalyst, the reaction is considered to be a cross-coupling reaction.<sup>[4]</sup> Again, the alkynes are believed to be involved in the second step of the catalytic cycle, i.e., in a *transmetalation* step with the arylpalladium(II) complex via an alkynylcopper intermediate generated in situ (Scheme 4).



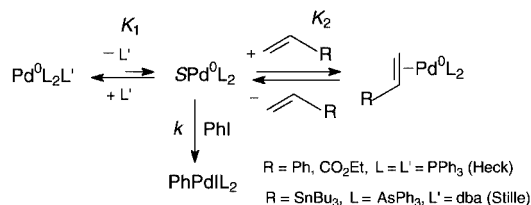
Scheme 4

In the copper-free process,<sup>[5]</sup> even if the origin of the alkynilide remains problematic, it is also believed to be involved in the second step of the catalytic cycle (*transmetalation*).

<sup>[a]</sup> Ecole Normale Supérieure, Département de Chimie, UMR CNRS-ENS-UPMC 8640, P.A.S.T.E.U.R. 24, Rue Lhomond, 75231 Paris, Cedex 5, France Fax: (internat.) + 33-1-4432-3325 E-mail: christian.amatore@ens.fr Anny.Jutand@ens.fr

<sup>[b]</sup> Université de Tlemcen, Faculté des Sciences, Département de Chimie, BP 119, M-13000 Tlemcen, Algérie

It has been established that in Heck reactions performed with alkenes (styrene, methyl acrylate)<sup>[6,7]</sup> or in Stille reactions performed with a vinyltin derivative ( $\text{CH}_2=\text{CH}-\text{SnBu}_3$ ),<sup>[8]</sup> the nucleophiles play a role before the *carbopalladation* (Heck reaction) or *transmetallation* (Stille reaction) steps, by having a decelerating effect on the oxidative addition. Indeed, the oxidative addition is slower in the presence of the nucleophile, because of a partial coordination of the active  $\text{Pd}^0$  complex by the  $\text{C}=\text{C}$  bond of the nucleophile, which results into unreactive  $\text{Pd}^0$  complexes (Scheme 5)<sup>[7,8]</sup> or very weakly reactive  $\text{Pd}^0$  complexes.<sup>[6]</sup>



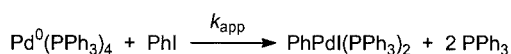
Scheme 5. Mechanism of the oxidative addition of PhI to  $[\text{Pd}^0]$  complexes in the presence of alkenes or vinyl(tributyl)tin in DMF

Consequently, we were interested in investigating the role of alkynes involved in palladium-catalyzed multicomponent (Scheme 1) or Sonogashira (Scheme 2) reactions toward the kinetics of the oxidative additions, because they possess a  $\text{C}\equiv\text{C}$  bond that is able to coordinate to  $\text{Pd}^0$  complexes. We report herein our investigations that generalize the role played by unsaturated nucleophiles in the kinetics of oxidative additions, i.e., before their implication in the classical carbopalladation or transmetallation steps.

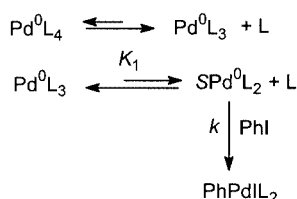
## Results and Discussion

### Oxidative Addition of PhI to $[\text{Pd}^0(\text{PPh}_3)_4]$ in DMF in the Presence of Phenylacetylene

The mechanism of the oxidative addition of PhI to  $[\text{Pd}^0(\text{PPh}_3)_4]$  (Scheme 6) is reported in Scheme 7.<sup>[9,10]</sup>



Scheme 6



Scheme 7. Mechanism of the oxidative addition of PhI to  $[\text{Pd}^0(\text{PPh}_3)_4]$  (S = solvent, L =  $\text{PPh}_3$ )

The corresponding kinetic law is given by Equation (1), where  $k_{\text{app}} = kK_1/[\text{L}]$

$$\frac{d[\text{Pd}^0]}{dt} = - \frac{kK_1[\text{PhI}][\text{Pd}^0]}{[\text{L}]} = -k_{\text{app}}[\text{PhI}][\text{Pd}^0] \quad (1)$$

with  $k_{\text{app}} = kK_1/[\text{L}]$

Under stoichiometric conditions, when  $[\text{PhI}] = [\text{Pd}^0(\text{PPh}_3)_4]_0 = c_0$ , the integration of Equation (1) gives Equation (2), where  $x = [\text{Pd}^0]_t/[\text{Pd}^0]_0$ .<sup>[11]</sup>

$$\frac{1}{x} = k_{\text{app}}c_0t + 1 \quad (2)$$

As reported, the kinetics of the oxidative addition of PhI to  $[\text{Pd}^0(\text{PPh}_3)_4]$  in DMF (containing  $n\text{Bu}_4\text{NBF}_4$ , 0.3 M) can be monitored by amperometry performed at a rotating disk electrode, polarized at +0.2 V vs. SCE, i.e., on the oxidation wave of  $[\text{Pd}^0(\text{PPh}_3)_3]$ <sup>[9,10]</sup> The decay of the oxidation current (proportional to the  $\text{Pd}^0$  concentration) was recorded versus time. The value of  $k_{\text{app}}$ , the apparent rate constant of the overall oxidative addition (Scheme 6), was then determined from the slope of the regression line obtained by plotting  $i_0/i = [\text{Pd}^0]_0/[\text{Pd}^0]_t = 1/x$  versus time [Equation (2), uppermost line in Figure 1];  $k_{\text{app}} = 24 \text{ M}^{-1} \text{ s}^{-1}$  ( $c_0 = 2 \text{ mM}$ ). The value of  $kK_1$  was also calculated:  $kK_1 = 0.062 \text{ s}^{-1}$  (DMF, 25 °C).<sup>[11]</sup>

When  $\text{PhC}\equiv\text{CH}$  (200 equiv.) was added to a solution of  $[\text{Pd}^0(\text{PPh}_3)_4]$  (2 mM) in DMF (containing  $n\text{Bu}_4\text{NBF}_4$ , 0.3 mM), the partial decay of the oxidation peak of  $[\text{Pd}^0(\text{PPh}_3)_3]$  at  $E_{\text{ox}}^p = +0.08 \text{ V}$  was observed together with a small shift toward more-positive potential (+0.10 V), which is indicative of a CE mechanism. No other oxidation peak was detected within the potential range investigated (up to +1 V). A  $^{31}\text{P}$  NMR spectrum of a solution of  $[\text{Pd}^0(\text{PPh}_3)_4]$  (12 mM) and  $\text{PhC}\equiv\text{CH}$  (2.4 M) in DMF (containing 10%  $[\text{D}_6]\text{acetone}$ ) exhibited, besides the broad signal of  $[\text{Pd}^0(\text{PPh}_3)_3]$  at  $\delta = 0.61 \text{ ppm}$ , two broad signals ( $\Delta\nu_{1/2} = 20 \text{ Hz}$ ) of the same magnitude at  $\delta = 25.44$  and 28.4 ppm, which are characteristic of two magnetically non-equivalent phosphane units. A new complex was then formed by addition of  $\text{PhC}\equiv\text{CH}$  to  $[\text{Pd}^0(\text{PPh}_3)_4]$  in DMF. The formation of a  $\text{Pd}^{\text{II}}$  complex by activation of the  $\text{C}-\text{H}$  bond, such as  $[\text{trans-PhC}\equiv\text{C}-\text{PdH}(\text{PPh}_3)_2]$ ,<sup>[12–14]</sup> is excluded because it would contain two magnetically equivalent phosphane units. Moreover, no signal that is characteristic of a hydride was detected by  $^1\text{H}$  NMR spectroscopy in  $\text{CDCl}_3$ .<sup>[12–14]</sup> Consequently, the new complex generated by addition of  $\text{PhC}\equiv\text{CH}$  to  $[\text{Pd}^0(\text{PPh}_3)_4]$  must result from complexation of the  $\text{C}\equiv\text{C}$  bond,  $[(\eta^2\text{-PhC}\equiv\text{CH})\text{Pd}^0(\text{PPh}_3)_2]$  (Scheme 8), as has been observed for alkenes (styrene, methyl acrylate).<sup>[7]</sup>  $[(\eta^2\text{-PhC}\equiv\text{CH})\text{Pd}^0(\text{PPh}_3)_2]$  was characterized by FAB mass spectrometry ( $m/z = 733 [\text{M} + \text{H}]^+$ ,  $630 [\text{M} - \text{PhC}\equiv\text{CH}]$ ).

The kinetics of the oxidative addition of PhI ( $c_0 = 2 \text{ mM}$ ) to  $[\text{Pd}^0(\text{PPh}_3)_4]$  ( $c_0 = 2 \text{ mM}$ ) in DMF in the presence of

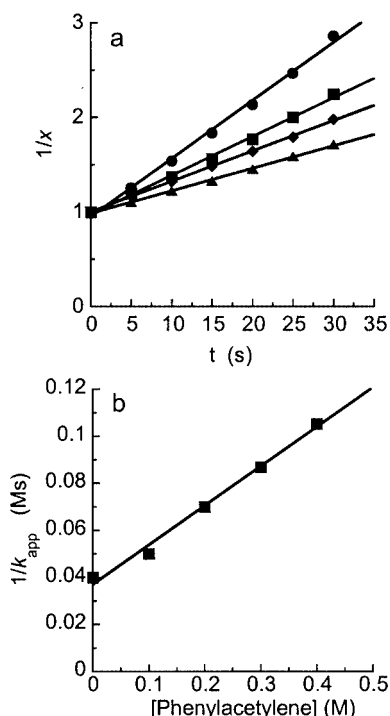
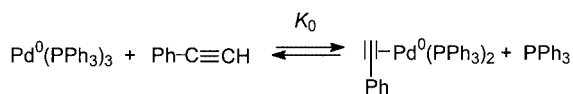
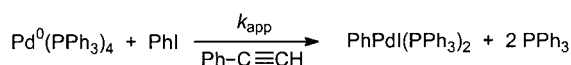


Figure 1. Oxidative addition of PhI (2 mM) to  $[\text{Pd}^0(\text{PPh}_3)_4]$  (2 mM) in DMF (containing  $n\text{Bu}_4\text{NBF}_4$  0.3 M), in the absence or presence of phenylacetylene, as monitored by amperometry at a rotating gold disk electrode (diameter: 2 mm;  $\omega = 105 \text{ rad s}^{-1}$ ) polarized at +0.2 V vs. SCE, at 25 °C. (a) Plot of  $1/x = i_0/i = [\text{Pd}^0]_0/[\text{Pd}^0]_t$  vs. time ( $i$  = intensity of the oxidation current of  $[\text{Pd}^0(\text{PPh}_3)_3]$  at  $t$ ;  $i_0$  = initial intensity of the oxidation current of  $[\text{Pd}^0(\text{PPh}_3)_3]$ ;  $1/x = k_{app}c_0t + 1$  [Equation (2)]). Oxidative addition performed in the absence of phenylacetylene (filled circles) and in the presence of phenylacetylene: (filled rectangle) 0.1; (filled trapezoid) 0.2; (filled triangle) 0.4 M. (b) Plot of  $1/k_{app}$  vs. concentration of phenylacetylene [Equation (5)]. The value of  $k_{app}$  was determined from the slope of the regression lines obtained in Figure 1, a



Scheme 8

various amounts of  $\text{PhC}\equiv\text{CH}$  (0.1–0.4 M) were investigated by amperometry (Scheme 9), as performed above in the absence of  $\text{PhC}\equiv\text{CH}$ .  $\text{PhC}\equiv\text{CH}$  was added to  $[\text{Pd}^0(\text{PPh}_3)_4]$  before the introduction of PhI.

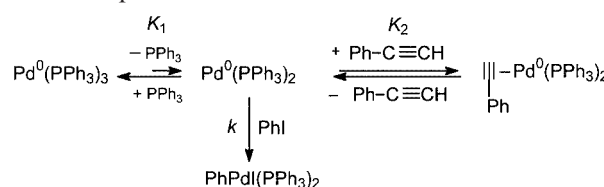


Scheme 9

The overall oxidative addition was slowed down in the presence of increasing amounts of phenylacetylene, as evidenced by the decay of the slopes of the plots of  $1/x$  versus time at the different  $\text{PhC}\equiv\text{CH}$  concentrations (Figure 1, a).

This behavior is similar to that already observed to occur in the presence of alkenes (styrene, methyl acrylate).<sup>[7]</sup> The occurrence of this process implies that the concentration of the active  $\text{Pd}^0(\text{PPh}_3)_2$  species decreases because of its reversible coordination by the alkyne, which generates the unreactive

complex,  $[(\eta^2\text{-PhC}\equiv\text{CH})\text{Pd}^0(\text{PPh}_3)_2]$ , according to the mechanism presented in Scheme 10.



Scheme 10. Mechanism of the oxidative addition of PhI to  $[\text{Pd}^0(\text{PPh}_3)_4]$  in DMF in the presence of phenylacetylene

For PhI and  $[\text{Pd}^0(\text{PPh}_3)_4]$  under stoichiometric conditions, a new kinetic law is expressed as in Equation (3) and (4).<sup>[15]</sup>

$$\frac{d[\text{Pd}^0]}{dt} = - \frac{kK_1[\text{PhI}][\text{Pd}^0]}{[\text{L}] + K_1K_2[\text{alkyne}]} \quad (3)$$

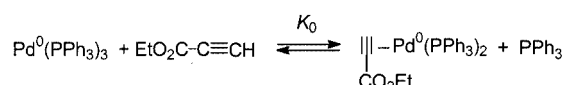
$$\frac{1}{x} = \frac{kK_1C_0t}{[\text{L}] + K_1K_2[\text{alkyne}]} + 1 = k_{app}C_0t + 1 \quad (4)$$

$$\frac{1}{k_{app}} = \frac{[\text{L}]}{kK_1} + \frac{K_2[\text{alkyne}]}{k} \quad (5)$$

The plot of  $1/k_{app}$  against the  $\text{PhC}\equiv\text{CH}$  concentration is linear (Figure 1, b) —  $1/k_{app} = 0.0369 + 0.167[\text{alkyne}]$  — which is in agreement with the mechanism of Scheme 10 and Equation (5). The value of  $[\text{L}]/kK_1 = 0.0369 \text{ Ms}$  was obtained from the intercept and that of  $K_2/k = 0.167 \text{ s}$  from the slope [Equation (5)]. Using  $[\text{L}] = 2.6 \text{ mM}$ ,<sup>[15]</sup> one obtains  $kK_1 = 0.07 \text{ s}^{-1}$ . This value allows the calculation of the equilibrium constant  $K_0$  for the overall equilibrium in Scheme 8 ( $K_0 = [(\eta^2\text{-alkyne})\text{Pd}^0\text{L}_2][\text{L}]/[\text{Pd}^0\text{L}_3][\text{alkyne}]$ ):  $K_0 = K_1K_2 = 0.012$  (DMF, 25 °C)

#### Oxidative Addition of PhI to $[\text{Pd}^0(\text{PPh}_3)_4]$ in DMF in the Presence of Ethylpropiolate, $\text{EtO}_2\text{C-C}\equiv\text{C-H}$

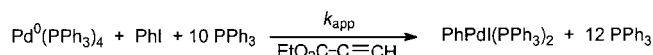
When two equiv. of  $\text{EtO}_2\text{C-C}\equiv\text{CH}$  (34 mM) were added to a solution of  $[\text{Pd}^0(\text{PPh}_3)_4]$  (17 mM) in  $[\text{D}_6]\text{acetone}$ , the  $^1\text{H}$  NMR spectrum exhibited two broad singlets at  $\delta = 4.21$  and 1.26 ppm instead of the triplet ( $\delta = 1.28 \text{ ppm}$ ,  $J = 7 \text{ Hz}$ , 3 H) and quadruplet ( $\delta = 4.23 \text{ ppm}$ ,  $J = 7 \text{ Hz}$ , 2 H), respectively that are characteristic of the  $\text{CH}_3\text{-CH}_2$  protons in the free alkyne,  $\text{EtO}_2\text{C-C}\equiv\text{C-H}$ . Similarly, the thin singlet of the C-H proton of free  $\text{EtO}_2\text{C-C}\equiv\text{CH}$  was no longer detected at  $\delta = 3.76 \text{ ppm}$ , but, instead, a broad singlet appeared at  $\delta = 2.86 \text{ ppm}$ . This feature establishes that  $\text{EtO}_2\text{C-C}\equiv\text{CH}$  is involved in an equilibrium with the initial  $\text{Pd}^0$  complex and results in average signals for the free and the coordinated  $\text{EtO}_2\text{C-C}\equiv\text{CH}$  (Scheme 11).



Scheme 11

A  $^{31}\text{P}$  NMR spectrum of  $[\text{Pd}^0(\text{PPh}_3)_4]$  (16 mM) in DMF (containing 10%  $[\text{D}_6]\text{acetone}$ ) exhibited, after addition of  $\text{EtO}_2\text{C}-\text{C}\equiv\text{CH}$  (0.16 M), a broad signal ( $\Delta\nu_{1/2} = 47$  Hz) for  $[\text{Pd}^0(\text{PPh}_3)_3]$  at  $\delta = -5.17$  ppm, i.e., very close to that of free  $\text{PPh}_3$  ( $\delta = -5.25$  ppm, not detected here), which indicates that the amount of  $[\text{Pd}^0(\text{PPh}_3)_3]$  in the equilibrium of Scheme 11 was very low. A second broad signal ( $\Delta\nu_{1/2} = 78$  Hz) was observed at  $\delta = 30.8$  ppm which we assign to  $[(\eta^2-\text{EtO}_2\text{C}-\text{C}\equiv\text{CH})\text{Pd}^0(\text{PPh}_3)_2]$  (Scheme 11). The equivalence of the two phosphane ligands in that complex may be due to a fast internal rotation of the alkyne ligand, which is in agreement with the broadening observed for the signals of the protons of the coordinated  $\text{EtO}_2\text{C}-\text{C}\equiv\text{CH}$  unit in the  $^1\text{H}$  NMR spectrum (vide supra).  $[(\eta^2-\text{EtO}_2\text{C}-\text{C}\equiv\text{CH})\text{Pd}^0(\text{PPh}_3)_2]$  was characterized by FAB mass spectrometry ( $m/z = 729$   $[\text{M} + \text{H}]^+$ ,  $630$   $[\text{M} - \text{EtCO}_2\text{C}\equiv\text{CH}]$ ).

When 1 equiv. of  $\text{EtO}_2\text{C}-\text{C}\equiv\text{CH}$  was added to a solution of  $[\text{Pd}^0(\text{PPh}_3)_4]$  (2 mM) in DMF (containing  $n\text{Bu}_4\text{NBF}_4$ , 0.3 M), the oxidation peak of  $[\text{Pd}^0(\text{PPh}_3)_3]$  at +0.08 V was no longer observed, which excluded a priori the investigation of the kinetics of the oxidative addition by amperometry. This problem was circumvented by the addition of excess  $\text{PPh}_3$  (10 equiv.), which shifted the equilibrium in Scheme 11 towards its left-hand side so that  $[\text{Pd}^0(\text{PPh}_3)_3]$  could be detected by its oxidation peak and, consequently, the kinetics of the oxidative addition could be monitored as above by amperometry. The kinetics of the oxidative addition of  $\text{PhI}$  ( $c_0 = 2$  mM) to  $[\text{Pd}^0(\text{PPh}_3)_4]$  ( $c_0 = 2$  mM) were then investigated in DMF in the presence of  $\text{PPh}_3$  (20 mM) both in the absence and presence (5 to 30 mM) of  $\text{EtO}_2\text{C}-\text{C}\equiv\text{CH}$  (Scheme 12).



Scheme 12

The oxidative addition became slower upon increasing the  $\text{EtO}_2\text{C}-\text{C}\equiv\text{CH}$  concentration. A saturation effect was observed, however, at high  $\text{EtO}_2\text{C}-\text{C}\equiv\text{CH}$  concentrations, as evidenced by the plot of  $1/k_{\text{app}}$  vs.  $[\text{EtO}_2\text{C}-\text{C}\equiv\text{CH}]$  (Figure 2). The value of  $1/k_{\text{app}}$  varied linearly with  $[\text{EtO}_2\text{C}-\text{C}\equiv\text{CH}]$  at low concentrations ( $< 0.012$  M), as had been observed for  $\text{PhC}\equiv\text{CH}$  (Figure 1, b), whereas it was constant at high concentrations ( $> 0.02$  M) (Figure 2).

This behavior suggests that at low concentrations,  $[\text{Pd}^0(\text{PPh}_3)_2]$  remained the major reactive species, but it was present at lower concentration because of its complexation to  $\text{EtO}_2\text{C}-\text{C}\equiv\text{CH}$ . At high concentrations of  $\text{EtO}_2\text{C}-\text{C}\equiv\text{CH}$ , when the  $[\text{Pd}^0(\text{PPh}_3)_2]$  concentration became very low as a result of the formation of  $[(\eta^2-\text{EtO}_2\text{C}-\text{C}\equiv\text{CH})\text{Pd}^0(\text{PPh}_3)_2]$  (the equilibrium depicted in Scheme 11), this latter, weakly reactive species was, nevertheless, sufficiently reactive to take over the role of active catalyst.  $[(\eta^2-\text{EtO}_2\text{C}-\text{C}\equiv\text{CH})\text{Pd}^0(\text{PPh}_3)_2]$  became the

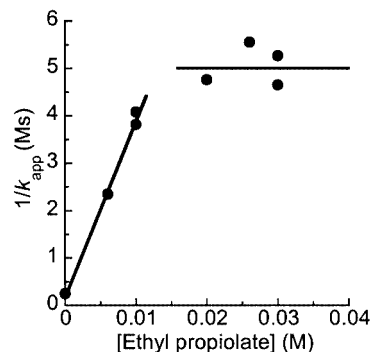
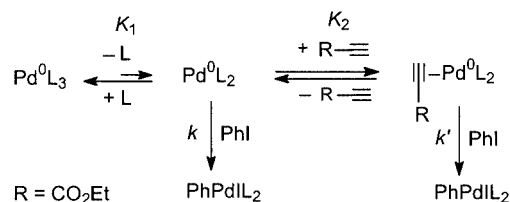


Figure 2. Oxidative addition of  $\text{PhI}$  (2 mM) to  $[\text{Pd}^0(\text{PPh}_3)_4]$  (2 mM) in DMF (containing  $n\text{Bu}_4\text{NBF}_4$  0.3 M) in the presence of  $\text{EtO}_2\text{C}-\text{C}\equiv\text{CH}$ , monitored by amperometry at a rotating gold disk electrode (i.d. 2 mm,  $\omega = 105 \text{ rad s}^{-1}$ ) polarized at +0.2 V vs. SCE, at  $25^\circ\text{C}$ . Plot of  $1/k_{\text{app}}$  vs. the concentration of ethyl propiolate

major reactive complex, once the equilibrium depicted in Scheme 11 was totally shifted to its right-hand side (Scheme 13).



Scheme 13. Mechanism of the oxidative addition of  $\text{PhI}$  to  $[\text{Pd}^0(\text{PPh}_3)_4]$  in DMF in the presence of ethyl propiolate ( $\text{L} = \text{PPh}_3$ )

According to Scheme 13, the kinetic law is given by Equation (6)–(8).<sup>[16]</sup>

$$\frac{d[\text{Pd}^0]}{dt} = - \frac{[\text{PhI}][\text{Pd}^0](k + k'K_2[\text{alkyne}])}{[\text{L}]/K_1 + K_2[\text{alkyne}]} \quad (6)$$

$$\frac{1}{x} = \frac{(k + k'K_2[\text{alkyne}])C_0t}{[\text{L}]/K_1 + K_2[\text{alkyne}]} + 1 = k_{\text{app}}C_0t + 1 \quad (7)$$

$$\frac{1}{k_{\text{app}}} = \frac{[\text{L}]/K_1 + K_2[\text{alkyne}]}{k + k'K_2[\text{alkyne}]} \quad (8)$$

At high concentrations of  $\text{EtO}_2\text{C}\equiv\text{C}-\text{H}$  ( $> 0.02$  M),  $K_2[\text{alkyne}] > [\text{L}]/K_1$  and  $k'K_2[\text{alkyne}] > k$ . Thus, one obtains Equation (9), where  $k' = 0.2 \text{ M}^{-1}\text{s}^{-1}$  (DMF,  $25^\circ\text{C}$ ), as determined from Figure 2.

$$\frac{1}{k_{\text{app}}} = \frac{1}{k'} \quad (9)$$

At low concentrations of  $\text{EtO}_2\text{C}\equiv\text{C}-\text{H}$  ( $< 0.012$  M),  $k'K_2[\text{alkyne}] < k$ , so that one obtains Equation (10), which is similar to Equation (4) that was established above for  $\text{PhC}\equiv\text{CH}$ .

$$\frac{1}{k_{\text{app}}} = \frac{[\text{L}]}{kK_1} + \frac{K_2[\text{alkyne}]}{k} \quad (10)$$



- [8] C. Amatore, A. Bucaille, A. Fuxa, A. Jutand, G. Meyer, A. Ndedi Ntepe, *Chem. Eur. J.* **2001**, *7*, 2134–2142.
- [9] J. F. Fauvarque, F. Pflüger, M. Troupel, *J. Organomet. Chem.* **1981**, *208*, 419–427.
- [10] C. Amatore, A. Jutand, F. Khalil, M. A. M'Barki, L. Mottier, *Organometallics* **1993**, *12*, 3168–3178.
- [11] In the absence of excess  $\text{PPh}_3$ , the variation of its concentration must be considered in the kinetic law [Equation (1)] whose integration gives Equation (2)':  $1/x + 0.5\ln x = 0.5kK_1t + 1$ . The value of  $kK_1$  was determined from the slope of the regression line obtained by plotting  $1/x + 0.5\ln x$  against time:  $kK_1 = 0.062 \text{ s}^{-1}$ . Since  $k_{\text{app}} = kK_1/[\text{L}] = 24 \text{ M}^{-1} \text{ s}^{-1}$  was obtained by application of the approximate Equation (2) (see text), Equation (2) can be considered as a good approximation with an average value for  $[\text{L}]$  of 2.6 mM. This value is not far from the average value of 3 mM for the concentration of  $\text{PPh}_3$ , which varies from the initial concentration of 2 mM to 4 mM at 100% conversion. Consequently, the simplified kinetic law in Equation (2) can be used with a value of 2.6 mM for the average concentration of  $\text{PPh}_3$  under our conditions.
- [12] Such a complex was generated by reacting  $[\text{Pd}^0(\text{PPh}_3)_4]$  with  $\text{PhC}\equiv\text{CH}$  at  $80^\circ\text{C}$ , i.e., upon more drastic conditions than that investigated here. See the reported by: G. A. Chukhadzhyan, Z. K. Evoyan, L. N. Melkonyan, *J. Gen. Chem.* **1975**, *45*, 1096–1098. For reviews, see refs.<sup>[13,14]</sup>.
- [13] V. V. Grushin, *Chem. Rev.* **1996**, *96*, 2011–2033.
- [14] K. K. Hii, in *Handbook of Organopalladium Chemistry for Organic Synthesis* (Ed.: E.-i. Negishi), Wiley-Interscience, New York, **2002**, vol. 1, p. 81–90.
- [15] Because of the complexity of the kinetic law in the presence of the alkyne, a constant value of  $[\text{L}]$  was considered for the integration of Equation (3) to be equal to its average value of 2.6 mM (see ref.<sup>[11]</sup>) for all reactions performed here ( $c_0 = 2 \text{ mM}$ ).
- [16] In this case,  $[\text{L}]$  is constant because  $\text{PPh}_3$  was added in excess before the introduction of  $\text{EtO}_2\text{C}-\text{C}\equiv\text{CH}$  and  $\text{PhI}$ .
- [17] C. Amatore, A. Jutand, *J. Organomet. Chem.* **1999**, *576*, 254–278.
- [18] D. T. Rosevear, F. G. Stone, *J. Chem. Soc., A* **1968**, 164–167.

Received October 2, 2003